Journal of Data Analytics and Intelligent Decision-making
Journal homepage: jdaid.qom.ac.ir
University of Qom

Statistically Constrained Economic Design of a VSSI X-bar Control Chart Considering Taguchi Loss Function

Farzad Amiri*[a], Navid Rafiei[b]

A. Industrial Engineering Department, Kermanshah University of Technology, Kermanshah, Iran.
B. Industrial Engineering Department, Kermanshah University of Technology, Kermanshah, Iran.

ARTICLEINFO

Keywords:
Fraud detection
Ensemble learning
Credit cards
Machine learning
Deep learning

ABSTRACT

The rapid growth of digital payment systems has heightened the need for accurate and scalable methods to detect credit card fraud. This study evaluates a range of machine learning and deep learning algorithms, including Logistic Regression, Decision Tree, Random Forest, K-Nearest Neighbors (KNN), XGBoost, Convolutional Neural Networks (CNN), Baseline MLP (Multi-Layer Perceptron), and Long Short-Term Memory (LSTM), to identify effective approaches for detecting fraudulent transactions. Based on comparative analysis, Random Forest and LSTM achieved the strongest individual performance, with accuracies exceeding 96%. Building on these findings, a stacking ensemble model was constructed by integrating Random Forest and LSTM as base learners and Logistic Regression as the meta-classifier. The framework incorporates Convolutional Autoencoder (CAE) for feature extraction and Random Undersampling (RUS) with three resampling ratios (1:1, 1:5, and 1:10) to address class imbalance. Experimental results indicated that the ensemble model provided improved predictive accuracy compared to individual algorithms, achieving an accuracy of 99.98%, a precision of 99.86%, and a recall of 99.89% under a 1:10 resampling ratio. Rather than proposing a new algorithmic architecture, this study contributes to a systematic and unified evaluation of widely used ML and DL approaches and demonstrates the effectiveness of integrating CAE, RUS, and a Random Forest–LSTM stacking ensemble in enhancing fraud detection performance.

* Corresponding author.
E-mail addresses: f.amiri@kut.ac.ir (F. Amiri), n.rafiei@iau-tnb.ac.ir (N. Rafiei)
Received 2 November 2025; Received in revised form 17 November 2025; Accepted 19 November 2025
Available online 16 December 2025
3115-8161
Cite this article: Amiri, F., Rafiei, N. (2025). Statistically Constrained Economic Design of a VSSI X-bar Control Chart Considering Taguchi Loss Function *Journal of Data Analytics and Intelligent Decision-making*, 1(3), 56-69.
https://doi.org/10.22091/jdaid.2025.14415.1017

Introduction

The primary function of a control chart is to help management detect process variations. The control chart scheme is known as fixed ratio sampling (FRS) when fixed sample sizes are obtained at fixed sampling intervals from the process. On the other hand, adaptive schemes that are practical tools for statistically monitoring the quality of products and processes can change dynamically over time, depending on the control chart statistic at each sampling instance (Saghir et al., 2023).

A control scheme can be designed from statistical, economic, or statistical-economic perspectives. The statistical view focuses on the chart's statistical performance. The financial view focuses on the economic impacts that a control scheme may have on the production of nonconforming items. However, the simultaneous implementation of economic and statistical perspectives helps a control scheme benefit from both criteria.

Researchers introduced adaptive control charts to enhance the performance of control schemes further. According to the literature, adaptive control schemes outperform FRS control schemes in terms of statistical and economic criteria due to the additional flexibility of the design parameters (Tang et al., 2019).

A control chart with adaptive sampling intervals was first introduced by Reynolds et al. (1988). In adaptive control charts, design parameters are allowed to vary depending on the value of the sample statistic. Four common types of adaptive schemes are widely discussed in the literature. These schemes are the variable sampling interval (VSI), variable sample size (VSS), variable sample size and sampling interval (VSSI), and variable parameters (VP) schemes. In the VSI scheme, the sampling interval for the following sample would be one of the two possible values (short or long sampling interval) based on the current position of the statistic plotted on the chart. In the VSS scheme, one can vary the size of the following sample depending on the current position of the chart's statistics. The VSSI scheme combines the VSS and VSI features into a single chart, which allows both the sample size and the sampling interval to vary. The VP scheme uses a full adaptive (FA) policy, which varies all design parameters when implementing the control chart (Ketabi and Khoo, 2021).

Considering that the primary focus of this paper is on VSSI-type adaptive schemes, a review of some studies in this field is mentioned. Khaw et al. (2017) proposed a coefficient of variation chart utilizing the VSSI feature to enhance the performance of the basic coefficient of variation chart, thereby facilitating the detection of small and moderate shifts in the coefficient of variation. Cheng and Wang (2018) presented a VSSI median control chart with estimated parameters in the presence of measurement errors for a normal process. A VSSI control chart using auxiliary information is proposed by Saha et al. (2019) for efficiently monitoring the process mean. Khoo et al. (2019) proposed an upper-sided improved VSSIt S chart by improving the existing upper-sided VSSI S chart through the inclusion of an additional sampling interval. A one-sided Downward control chart for monitoring the multivariate coefficient of variation with VSSI Strategy considered by Chew and Khaw (2020). Yeong et al. (2024) improved the sensitivity of the existing run sum chart for shifts in the coefficient of variation by proposing two types of adaptive schemes, i.e., the VSSI and VP schemes. An improved variable parameter mean square error control chart is proposed by Chen (2023), which utilizes three different sampling intervals, two different sample sizes, and two different control limits.

In practice, when implementing a control chart, three design parameters need to be determined in advance: the sample size (n), the sampling interval between successive samples (h), and the control limits' coefficient (k). Thus, designing a control chart involves selecting these parameters. There are three approaches in the literature for designing a control chart: statistical design, economic design, and economic statistical design (Rafiei and Asadzadeh,

2022). Duncan (1956) proposed the first economic design model to determine control chart parameters in the presence of an assignable cause, aiming to minimize the average cost. Another popular model was developed by Lorenzen and Vance (1986), which offers greater flexibility than Duncan's model.

To improve the statistical properties of an economically designed control chart, Saniga (1989) added Type I and Type II errors as constraints to Duncan's model. His study laid the foundation for another approach to designing control charts, known as the economic statistical design. (Ketabi et al., 2017) investigated the economic and economic statistical designs of the SVSSI T2 charts and utilized the Markov chain approach to develop the cost model proposed by Costa and Rahim. Ghanaatiyan et al. (2017) proposed a multi-objective model for the economic-statistical design of the VSSI multivariate EWMA control chart by using double warning lines. Chew et al. (2022) investigated the economic and economic-statistical performances of the VSSI coefficient of variation chart. Mirabi et al. (2021) considered the economic-statistical design of the VSSI X-bar control chart with multiple assignable causes. Ketabi and Khoo (2021) developed an economic statistical model for the VSSI multivariate T2 control chart. To improve the monitoring efficiency of the multivariable autocorrelation process and reduce the cost of process control, Xue et al. (2025) proposed an economic statistical design method for residual Multivariate EWMA control charts with variable VSSIs.

Additionally, several researchers have applied the Taguchi loss function approach in designing control charts (Yu and Chen, 2009; Amiri et al., 2024; Huang, 2023). Taguchi's loss function considers the loss incurred as a result of deviating from the target value. The greater the deviation from the target value, the greater the loss incurred and imposed on society. This aligns with the primary principle of the Six Sigma methodology, which is to minimize deviations from the target value (Yu and Chen, 2009). To the best of our knowledge, the statistically constrained economic design of a VSSI X-bar control chart considering the Taguchi loss function has rarely been considered in the literature. In this paper, we develop a statistically constrained economic design for a VSSI X-bar control chart based on the statistical measures AATS and ANF, as well as the economic measure of hourly cost.

The remainder of this paper is organized as follows. In section 2, the Taguchi loss function is introduced. The VSSI control chart is developed in Section 3. Section 4 describes the proposed solution algorithm. In Section 5, an illustrative example is given, and a comparison with the FRS scheme is investigated in Section 6. Our concluding remarks are provided in the final section.

Theoretical Foundations and Research Background

From Taguchi's perspective, the loss incurred by a product is associated with any deviation of a quality characteristic from its target value. The purpose of a loss function is to reflect the economic loss related to variations in and deviations from the process target or the target value of a product characteristic. Reduction in the dispersion of the distribution around the target value is equivalent to lower loss and higher quality. Jiao and Helo (2008) studied an optimization design of a CUSUM control chart based on Taguchi's loss function. Yu and Chen, (2009) proposed an economic statistical design of X-bar control charts using Taguchi loss functions. Niaki et al. (2010) studied the economic-statistical designs of multivariate EWMA control charts using the multivariate Taguchi loss approach. Safaei et al. (2012) studied a multi-objective model of the economic statistical design of the X-bar control chart, incorporating the Taguchi loss function and intangible external costs. Amiri et al. (2014) considered the Taguchi loss function for the economic-statistical design of an adaptive X-bar control chart.

Furthermore, Huang (2023) developed an economical design of the Max chart based on a unified model and embellished it with Taguchi's quality loss function. In this paper, the Taguchi

loss function is considered as L(X) = K (X - T)2, where X is a key quality characteristic, K is a positive coefficient, and T is the target. Suppose the specification limits for a quality characteristic are T ± Δ, and it costs A to rework or scrap one unit of the product. The coefficient K of the loss function can then be stated as K = A / Δ2 (Amiri et al., 2014).

When the process is in control, the mean and variance of X are μ0 and σ02, respectively. Suppose the probability density function of the quality characteristic denoted by denoted by f(x) follows N (μ0, σ02). It is desired for the target value (T) to be equal to the in-control mean μ0. However, if μ0 differs from the target value T, a fixed bias affects all manufactured items. Then, the expected quality cost per unit of the product when the process is in control, J0, is given in Equation (1) (Safaei et al., 2012).

$$\begin{aligned} J_0 &= \int_{-\infty}^{+\infty} K(x-T)^2 f(x)dx = \int_{-\infty}^{+\infty} K(x-\mu_0+\mu_0-T)^2 f(x)dx \\ &= K\left[\sigma_0^2 + (\mu_0 - T)^2\right] \end{aligned} \tag{1}$$

When an assignable cause occurs, the out-of-control process mean will be μ1 = μ0 + δσ0, and the expected quality cost per unit when the process shifts to an out-of-control state, J1, is

$$\begin{aligned} J_1 &= \int_{-\infty}^{+\infty} K(x-\mu_1+\mu_1-T)^2 f(x)dx \\ &= \int_{-\infty}^{+\infty} K(x-\mu_0-\delta\sigma_0+\mu_0+\delta\sigma_0-T)^2 f(x)dx \\ &= K\left[\sigma_0^2 + (\mu_0-T)^2 + \delta^2\sigma_0^2 - 2\delta\sigma_0(\mu_0-T)\right] \end{aligned} \tag{2}$$

VSSI scheme

To monitor a process using a control chart, the values of four parameters must be determined: the sample size (n), the sampling interval (h), the warning limits coefficient (w), and the control limits coefficient (k). Usually, two sampling intervals, h2 < h1, and two sample sizes, n1 < n2, are used. The size of the sample and the sampling interval are established based on the position of the current sampling statistic on the chart. In this regard, if the current sample mean falls in the warning region, the design (n2, h2, k, w) should be used for the next sample. Alternatively, if the current sample point falls in the central region, the chart design (n1, h1, k, w) should be employed for the next sample.

Adjusted average time from the process mean shift until the chart produces a signal (AATS) is the statistical measure to determine how fast a control chart detects a process mean shift. Moreover, the average time of the cycle (ATC) is the average time from the start of the production till the first signal after the process shift. If the assignable cause occurs according to an exponential distribution with parameter λ, then the expected time interval that the process remains in control is 1/λ. The memoryless property of the exponential distribution allows the computation of the ATC using the Markov chain approach (Pourtaheri, 2021). Hence, AATS can be determined using Equation (3).

$$AATS = ATC - \frac{1}{\lambda} \tag{3}$$

Moreover, in the VSSI scheme, when n1 = n2 = n and h2 < h1 then the VSSI X-bar chart simplifies to the VSI X-bar chart. When n1 < n < n2 and h1 = h2 = h, the VSSI X-bar chart reduces to the VSS X-bar chart.

Markov chain approach

According to the VSSI scheme, at each sampling stage, one of the following transient states is met, depending on the process status (in-control or out-of-control), sample size (small or large), and sampling interval (short or long). Faraz and Saniga (2011) provided some unifying definitions of the Markov chain approach in designing adaptive control charts. The process states could be defined as follows. The process is in state one if the current sample point falls in the central region if the process is in control.

State 1: $|Z| \leq w$ and the process is in control;

State 2: $w < |Z| \leq k$ and the process is in control;

State 3: $|Z| \leq w$ and the process is out of control;

State 4: $w < |Z| \leq k$ and the process is out of control;

If a sample statistic falls in the action region at the time of sampling,, i.e., $|Z| > k$, when the process is out of control, then an actual alarm is signaled, and the absorbing state, i.e. state 5, is reached. To model the VSSI scheme using a Markov chain approach, the transition probabilities pij should be defined, where i and j denote the prior and current states, respectively. The transition probability matrix is given as follows (Faraz and Saniga, 2011; Rafiei et al., 2023).

$$\mathbf{P} = \begin{bmatrix} p_{11} & p_{12} & p_{13} & p_{14} & p_{15} \\ p_{21} & p_{22} & p_{23} & p_{24} & p_{25} \\ 0 & 0 & p_{33} & p_{34} & p_{35} \\ 0 & 0 & p_{43} & p_{44} & p_{45} \\ 0 & 0 & 0 & 0 & 1 \end{bmatrix} \quad (4)$$

where

$$
\begin{aligned}
p_{11} &= \Pr(|Z| \le w \,||Z| \le k) \times e^{-\lambda h_1} = (\Phi(w) - 0.5)/(\Phi(k) - 0.5) \times e^{-\lambda h_1} \\
p_{12} &= \Pr(w < |Z| \le k \,||Z| \le k) \times e^{-\lambda h_1} = (\Phi(k) - \Phi(w))/(\Phi(k) - 0.5) \times e^{-\lambda h_1} \\
p_{13} &= \Pr(|Y| \le w \,|Y \sim N(\delta\sqrt{n_1}, 1)) \times (1 - e^{-\lambda h_1}) \\
&= \left[\Phi(w - \delta\sqrt{n_1}) - \Phi(-w - \delta\sqrt{n_1})\right] \times (1 - e^{-\lambda h_1}) \\
p_{14} &= \Pr(w < |Y| \le k \,|Y \sim N(\delta\sqrt{n_1}, 1)) \times (1 - e^{-\lambda h_1}) \\
&= \left[\Phi(k - \delta\sqrt{n_1}) - \Phi(-k - \delta\sqrt{n_1}) - \Phi(w - \delta\sqrt{n_1}) + \Phi(-w - \delta\sqrt{n_1})\right] \\
&\times (1 - e^{-\lambda h_1}) \\
p_{15} &= \Pr(|Y| \ge k \,|Y \sim N(\delta\sqrt{n_1}, 1)) \times (1 - e^{-\lambda h_1}) \\
&= \left[1 - \Phi(k - \delta\sqrt{n_1}) + \Phi(-k - \delta\sqrt{n_1})\right] \times (1 - e^{-\lambda h_1}) \\
p_{21} &= \Pr(|Z| \le w \,||Z| \le k) \times e^{-\lambda h_2} = (\Phi(w) - 0.5)/(\Phi(k) - 0.5) \times e^{-\lambda h_2} \\
p_{22} &= \Pr(w < |Z| \le k \,||Z| \le k) \times e^{-\lambda h_2} = (\Phi(k) - \Phi(w))/(\Phi(k) - 0.5) \times e^{-\lambda h_2} \\
p_{23} &= \Pr(|Y| \le w \,|Y \sim N(\delta\sqrt{n_2}, 1)) \times (1 - e^{-\lambda h_2}) \\
&= \left[\Phi(w - \delta\sqrt{n_2}) - \Phi(-w - \delta\sqrt{n_2})\right] \times (1 - e^{-\lambda h_2}) \\
p_{24} &= \Pr(w < |Y| \le k \,|Y \sim N(\delta\sqrt{n_2}, 1)) \times (1 - e^{-\lambda h_2}) \\
&= \left[\Phi(k - \delta\sqrt{n_2}) - \Phi(-k - \delta\sqrt{n_2}) - \Phi(w - \delta\sqrt{n_2}) + \Phi(-w - \delta\sqrt{n_2})\right] \\
&\times (1 - e^{-\lambda h_2}) \\
p_{25} &= \Pr(|Y| \ge k \,|Y \sim N(\delta\sqrt{n_2}, 1)) \times (1 - e^{-\lambda h_2}) \\
&= \left[1 - \Phi(k - \delta\sqrt{n_2}) + \Phi(-k - \delta\sqrt{n_2})\right] \times (1 - e^{-\lambda h_2}) \\
p_{33} &= \Pr(|Y| \le w \,|Y \sim N(\delta\sqrt{n_1}, 1)) = \left[\Phi(w - \delta\sqrt{n_1}) - \Phi(-w - \delta\sqrt{n_1})\right] \\
p_{34} &= \Pr(w < |Y| \le k \,|Y \sim N(\delta\sqrt{n_1}, 1)) \\
&= \left[\Phi(k - \delta\sqrt{n_1}) - \Phi(-k - \delta\sqrt{n_1}) - \Phi(w - \delta\sqrt{n_1}) + \Phi(-w - \delta\sqrt{n_1})\right] \\
p_{35} &= \Pr(|Y| \ge k \,|Y \sim N(\delta\sqrt{n_1}, 1)) = 1 - \Phi(k - \delta\sqrt{n_1}) + \Phi(-k - \delta\sqrt{n_1}) \\
p_{43} &= \Pr(|Y| \le w \,|Y \sim N(\delta\sqrt{n_2}, 1)) = \Phi(w - \delta\sqrt{n_2}) - \Phi(-w - \delta\sqrt{n_2}) \\
p_{44} &= \Pr(w < |Y| \le k \,|Y \sim N(\delta\sqrt{n_2}, 1)) \\
&= \Phi(k - \delta\sqrt{n_2}) - \Phi(-k - \delta\sqrt{n_2}) - \Phi(w - \delta\sqrt{n_2}) + \Phi(-w - \delta\sqrt{n_2}) \\
p_{45} &= \Pr(|Y| \ge k \,|Y \sim N(\delta\sqrt{n_2}, 1)) = 1 - \Phi(k - \delta\sqrt{n_2}) + \Phi(-k - \delta\sqrt{n_2})
\end{aligned}
\tag{5}
$$

and Φ( ) is the cumulative probability distribution function of a standard normal random variable. In addition, Y ~ N(μ, σ2) denotes that is a normally distributed random variable with mean μ and variance σ2.

The product of the average number of instances a transient state is reached and the corresponding sampling interval determines the period ATC (Amiri et al., 2014; Faraz and Saniga, 2011).

$$ATC = \mathbf{b}'(\mathbf{I} - \mathbf{Q})^{-1}\mathbf{h} \tag{6}$$

where I is the identity matrix of order four; $\mathbf{b}' = (p_{11}, p_{12}, 0, 0)$ is a vector of initial. In this paper, the vector $\mathbf{b}'$ is set to (0, 1, 0, 0) to provide extra protection and prevent problems that

may arise during start-up. The matrix $\mathbf{Q}$ is the transition matrix without the elements associated with the absorbing state. Vector $\mathbf{h}' = (h_1, h_2, h_2, h_1)$ the vector of sampling intervals corresponding to the transient states. The average number of sampled items in the VSSI scheme is calculated using (Amiri et al., 2014; Faraz and Saniga, 2011):

$$ANI = \mathbf{b}'(\mathbf{I} - \mathbf{Q})^{-1}\boldsymbol{\eta} \tag{7}$$

where, $\boldsymbol{\eta}' = (n_1, n_2, n_2, n_1)$ is the vector of sample sizes corresponding to the transition states. (Faraz and Saniga, 2011), as well as others (Amiri et al., 2014), state that a meaningful comparison can be made between FRS and VSSI charts when the in-control performances of the charts are approximately the same. Hence, the same average number of items should be inspected during the in-control period for both schemes. Considering Markov chain properties, (Faraz and Saniga, 2011) calculated ANI as follows for the VSSI scheme.

$$ANI = \mathbf{b}'(\mathbf{I} - \mathbf{Q})^{-1}(n_1, n_2, 0, 0) \tag{8}$$

The expected number of false alarms per cycle is given in Equation (9) (Faraz and Saniga, 2011).

$$ANF = \mathbf{b}'(\mathbf{I} - \mathbf{Q})^{-1}\mathbf{f} \tag{9}$$

where $\mathbf{f} = (\alpha, \alpha, 0, 0)$ is the vector of false alarm probabilities in each transition state, and α is the probability of type I error when the chart has design parameters (ni, hi, k, w). When a false alarm is detected, an investigation begins, which reveals the nature of the alarm and allows the process to return to its in-control condition. Thus, the probability of a transition thereafter to any of the states equals the respective likelihood of states 1 and 2, as if no alarm had been generated. For the same reason, even if the signal reveals an actual occurrence of the assignable cause, the assignable cause will be immediately removed, and the process will then resume its in-control operation. Consequently, the probability of a transition to any state equals the respective likelihood of states 1 and 2 as if no cause had occurred. Finally, the product of the average number of instances a transient state has been reached and the corresponding false alarm rate determines the average number of false alarms.

Cost Model

Following the renewal reward process assumption, the expected quality cost per hour is computed as the ratio of expected cost per cycle to the expected cycle time. A quality cycle consists of one period when the process is in control and two periods during an out of control state. The expected length of the quality cycle is calculated as follows (Amiri et al., 2014).

$$ET = ATC + T_0 \times ANF + T_1 \tag{10}$$

The component ET is composed of the in control portion (including interruptions for false alarms; T0 is the average time to search when the process is in control), and T1 is the time to locate and repair the process.

The costs of producing nonconformities, whether the process is in control or out of control, as well as sampling and inspection costs, costs of false alarms, and costs of locating and repairing the assignable cause, are all elements of the expected cost per cycle. Each cost element is derived as follows (Amiri et al., 2022).

$$EC = C_0(1/\lambda) + C_1 \times (AATS) + s \times ANI + f_0 \times ANF + W \tag{11}$$

where, s is the sampling cost, f0 is the cost of a false alarm, and W is the cost to locate and repair the process.

Moreover, C0 and C1 represent the expected costs of producing non-conformities when the process is in control and out of control, respectively. If p units are produced per hour, C0 and C1 in the cost function (according to equations (1) and (2)) can be computed as C0 = J0p and C1=J1p. The expected cost per hour incurred by the process can be obtained as (Rafiei and Asadzadeh, 2022; Rafiei et al., 2023).

$$EA = \frac{EC}{ET} \tag{12}$$

In the economic-statistical design of the X-bar control chart VSSI scheme, the design vector is (n1, n2, h1, h2, k, w). The objective is to find a design vector that minimizes EA subject to some constraints. Hence, the optimization problem is defined as follows.

$$\begin{aligned} &Min \quad EA(n_1, n_2, h_1, h_2, k, w) \\ &\text{Subjec to :} \\ &ANF \le ANF_M \\ &AATS \le AATS_M \\ &h_{\min} \le h_2 < h_1 \le h_{\max} \\ &0 < w < k \le k_{\max} \\ &1 \le n_1 < n_2 \le n_{\max} \quad \text{(integers)} \end{aligned} \tag{13}$$

In the optimization model, the constraint ANF ≤ ANFM is added to provide the best protection against false alarms and AATS ≤ AATSM is added to detect process shifts as quickly as possible.

The minimum and maximum values of possible sampling intervals between successive samples, $h_{\min}$ and $h_{\max}$ are added to make the chart more practical. In this research, the values of hmin = 0.1 and hmax = 8 are used. Such intervals are also recommended by other researchers (Faraz and Saniga, 2011). Because the sampling intervals less than 0.1 and greater than 8 hours may be awkward in a work shift.

Solution Algorithm

The economic-statistical optimization model features both discrete and continuous decision variables, and genetic algorithm (GA) is employed in several research publications to optimize this problem (Rafiei and Asadzadeh, 2022; Xue et al., 2025; Amiri et al., 2014). The objective of GA is to obtain a globally optimum solution. GA starts to generate a new generation or population using a collection of small possible solutions in a parallel process. The quality of the solutions presented by GA depends on GA parameters. GA parameters are population Size (Npop), crossover (CP), number of elites (NE), number of generations (GN), and mutation rate. GA and the key parameters which should be determined at the beginning of the algorithm and should be used while applying the algorithm are described in the following steps:

1. GA starts to work using some possible initial solutions named "Initial Population." Each population has Npop chromosomes, which are produced from the solution. In this research, each chromosome consists of five genes; each representing a decision variable. The decision variable of the model includes (n1, n2, h1, h2, k, w).
2. The population will be evaluated based on the cost function and statistical constraints. The best chromosomes will be selected for crossover purposes. Chromosomes imported from the evaluation step will serve as inputs to the crossover operation, with a crossover fraction (CF) set to 0.5 (this value was determined using a Taguchi orthogonal array).
3. The elitism operator is a method for maintaining the best chromosomes of each generation. Elites of each generation will be transferred directly to the next generation to prevent the loss of the best chromosomes.
4. A mutation operator is employed to prevent GA from converging into a local optimum value. Selected chromosomes for mutation are not among the best of each generation.
5. After the mutation, the cost function and statistical constraints for each chromosome will be calculated. Then, the chromosomes will be ranked. The stopping criterion, the number of iterations in the algorithm, will be investigated, and the loop will continue until an optimized solution is achieved.

In the algorithm developed in this research, the mutation rate is considered a linear combination of the other parameters. The optimized values for four GA parameters are determined using the Taguchi orthogonal array. An L9 orthogonal array will consider nine combinations of control parameters at three different levels. Table (1) shows the value for each of the parameters.

Table 1. Levels for each of the model parameters

Parameter	Range	Level 1	Level 2	Level 3
Population size (N_{pop})	100 – 900	100	500	900
Crossover Fraction (CF)	0.1 – 0.9	0.1	0.50	0.90
Number of Elites (NE)	4 – 10	4	6	10
Number of Generations (NG)	50 – 150	50	100	150

The algorithm was iterated three times (Y1, Y2, and Y3) for each level, and results were obtained by running the algorithm 27 times in total. Since the objective function is to minimize, the smallest signal-to-noise ratio (SNR) is calculated to evaluate the experimental results.

$$SN = -10 \log\left(\frac{1}{r}\sum_{i=1}^{r} Y_i^{\,2}\right) \tag{14}$$

In equation (14), r is the number of replicates for each level. Solution and SN values for each level of parameters are tabulated in Table (2). The sum of the SN ratio for each of the three levels of the GA parameters is shown in Table (3). An optimized combination of four GA parameters, Npop = 900, CF = 0.5, NE = 6, and NG = 100, is recommended based on the maximum SN value for each parameter level.

Table 2. The objective values for each levels of GA parameters

Runs	N_{pop}	CF	NE	NG	Y1	Y2	Y3	SN
1	100	0.10	2	50	116.838	116.869	116.838	-41.3525
2	100	0.50	6	100	116.810	116.815	116.797	-41.3494

3	100	0.90	10	150	116.823	116.858	116.823	-41.3514
4	500	0.10	6	150	116.836	116.797	116.797	-41.3496
5	500	0.50	10	50	116.810	116.798	116.810	-41.3493
6	500	0.90	2	100	116.810	116.810	116.810	-41.3496
7	900	0.10	10	100	116.798	116.797	116.797	-41.3487
8	900	0.50	2	150	116.797	116.810	116.797	-41.3489
9	900	0.90	6	50	116.798	116.810	116.810	-41.3493

Table 3. The sum of SN ratio for each level of GA parameters

	Npop	CF	NE	NG
Level 1	-124.0533	-124.0507	-124.0510	-124.0511
Level 2	-124.0485	-124.0476*	-124.0483*	-124.0476*
Level 3	-124.0469*	-124.0503	-124.0494	-124.0499
*largest sum of SN ratio for each parameter within different levels [15]				

Numerical Analysis

To illustrate the application of the developed VSSI X-bar control chart, a numerical analysis is performed. The logical ranges for each of the control chart parameters, including sample size, sampling interval, and control limit coefficient, are considered to be [1, 30], [0.1, 8], and [1, 5], respectively. Cost and process parameters are defined as sampling cost s = $5, cost of detecting a reasonable deviation, W = $1000, cost of a false signal, f0 = $1500, the average time to search for the false signal is T0 = 5 hour, the average time to detect deviations and modify the process is T1 = 2 hours, and process mean increases by 1.5 standard deviations ($\delta = 1.5$).

Additionally, the quadratic loss function coefficient is set to K = 1. The actual process average equals the characteristic's target value, and the process variance is $\sigma 02 = 1$. The average process in-control period is equal to 100. If the production rate is equal to Pr = 100 units per hour, the production cost for each defective product, whether the process is in control or out of control is equal to C0 = 100J0 and C1 = 100J1, respectively.

The optimal parameters for fixed ratio sampling are (n, h, k)FRS = (6, 5, 2.71), which yields a cost of 122.09$ per hour, as well as ANFFRS = 0.14 and AATSFRS = 3.52 hours. Similarly, the optimal parameters for the economic-statistical design of the VSSI scheme are obtained as n1 = 3, n2 = 6, h1 = 3.75, h2 = 0.1, k = 3.49 and w = 1.50, giving the minimum cost per hour equal to $118.90, ANFVSSI = 0.02 and AATSVSSI = 2.69 hours.

Comparison of the adaptive schemes to the FRS scheme proves the efficiency of the proposed model. There is a 2.6% reduction in cost when the VSSI scheme is used. Furthermore, the average number of false signals is decreased. The AATSFRS of 3.52 hours is improved to AATSVSSI of 2.69 hours, indicating a 23.58% improvement. Given that a control chart may be designed to detect a variety of shift sizes in the process mean, other shift sizes are also examined.

Comparisons

In this section, the effect of shifts $\delta \in \{0.5, 1.0, 1.5, 2.0, 2.5\}$ in the process mean will be evaluated. To provide a fair comparison of FRS charts and variable ratios charts, statistical constraints ANF ≤ ANFM and AATS ≤ AATSM are removed in the computations of different schemes.

The optimum values for FRS, VSS, VSI, and VSSI schemes have been evaluated for different process mean shift sizes. The effect of the process mean shift on the optimum values of FRS and different adaptive schemes are summarized in Tables (4) to (7). As it is shown in Table (4), the corresponding cost for small process mean shifts is less than the cost for larger

shift values. However, the proposed model offers better AATS for lager shift values which results in the early identification of the assignable causes.

Table 4. Optimum solution of the VSSI scheme

δ	n1	n2	h1	h2	k	w	ANF	AATS	EA
0.5	1	22	8.00	8.00	2.65	1.20	0.11	44.23	116.80
1.0	4	10	6.64	0.10	3.27	1.30	0.02	6.17	118.30
1.5	3	6	3.75	0.10	3.49	1.50	0.02	2.69	118.90
2.0	2	4	2.27	0.10	3.61	1.61	0.02	1.56	119.36
2.5	1	3	1.24	0.10	3.75	1.61	0.02	1.02	119.56

Table 5. Optimum solutions of FRS scheme

δ	n	h	k	ANF	AATS	EA
0.5	6	8.00	2.31	0.27	53.53	117.85
1.0	10	8.00	2.53	0.15	6.91	120.89
1.5	6	4.99	2.71	0.14	3.53	122.09
2.0	4	3.04	2.91	0.12	2.01	122.89
2.5	3	2.12	3.08	0.10	1.31	123.46

Table 6. Optimum solutions of the VSI scheme

δ	n1	n2	h1	h2	k	w	ANF	AATS	EA
0.5	6	6	8.00	8.00	2.31	1.39	0.27	53.53	117.85
1.0	7	7	8.00	0.10	2.93	1.28	0.06	5.96	118.96
1.5	4	4	4.48	0.10	3.16	1.36	0.04	2.88	119.61
2.0	3	3	2.85	0.10	3.37	1.61	0.03	1.67	120.32
2.5	2	2	1.86	0.10	3.43	1.64	0.04	1.10	120.69

Table 7. Optimum solution of the VSS scheme

δ	n1	n2	h1	h2	k	w	ANF	AATS	EA
0.5	2	23	8.00	8.00	2.66	1.30	0.10	42.72	116.81
1.0	8	13	8.00	8.00	2.56	1.47	0.14	7.49	120.61
1.5	6	8	5.03	5.03	2.77	1.87	0.11	3.49	121.98
2.0	4	5	3.05	3.05	2.95	2.03	0.11	2.00	122.80
2.5	3	4	2.12	2.12	3.12	2.35	0.09	1.31	123.41

The optimum cost and AATS for different shift sizes in the process mean are shown in Figure (1) and Figure (2), respectively. Within the variable sampling schemes, VSS has the closest performance to the FRS scheme. Comparisons of different schemes indicate that the optimum solution for the VSSI scheme is always better than the other scheme from both cost and statistical viewpoints.

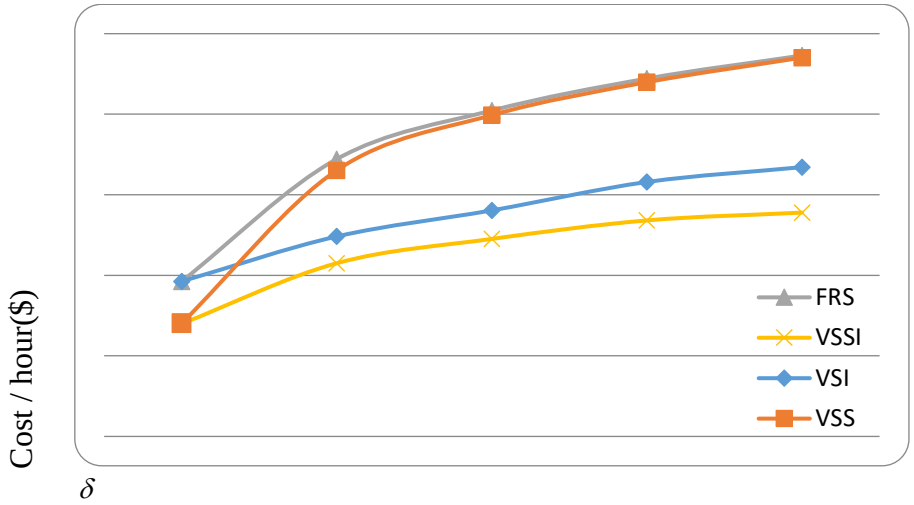

Figure 1. Comparison of cost in FRS and Variable ratio schemes

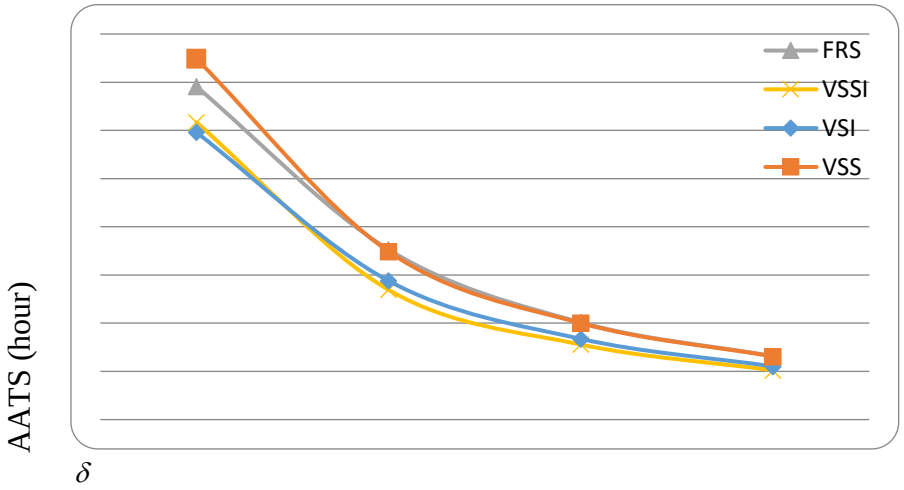

Figure 2. Comparison of AATS index of FRS and Variable ratio schemes

Conclusions

In this paper, variable sample size and variable sampling interval X-bar control charts are developed to monitor the process mean. Additionally, the relationship between process monitoring costs and deviations from the target value specified in technical specifications was incorporated into the model using the Taguchi quality loss function. Assessment of the optimized solutions reveals that changes in the shift size of the process mean impact both the average expected cost and the average time of an out-of-control alarm. The results of comparing variable sampling ratio with fixed sampling ratio schemes show that the proposed models identify the assignable cause sooner than the FRS scheme and are better in both expected cost of quality cycle and statistical performance. The interesting area worthy of continued research efforts includes the economic-statistical design of various VSSI charts in the presence of both fixed and variable competing risks. Furthermore, the economic and economic-statistical performances of various VSSI charts, such as EWMA and CUSUM, can also be studied in sensitive areas, including healthcare.

References

Amiri, F., Noghondarian, K. and Noorossana, R. (2014). "Economic-statistical design of adaptive X-bar control chart: a Taguchi loss function approach", Scientia Iranica, Vol. 21, No. 3, pp.1096-1104.

Chen, P.L. (2023). "An improved variable parameter mean square error control chart", Communications in Statistics-Theory and Methods, Vol. 52 No. 16, pp.5752-5766. https://doi.org/10.1080/03610926.2021.2019769

Cheng, X.B. and Wang, F.K. (2018). "VSSI median control chart with estimated parameters and measurement errors", Quality and Reliability Engineering International, Vol. 34, No. 5, pp.867-881. https://doi.org/10.1002/qre.2297

Chew, X. and Khaw, K.W. (2020). "One-sided downward control chart for monitoring the multivariate coefficient of variation with VSSI strategy", Journal of Mathematical and Fundamental Sciences, Vol. 52 No. 1, pp.112-130. https://doi.org/10.5614/j.math.fund.sci.2020.52.1.8

Chew, Y., Khoo, M.B., Khaw, K.W. and Yeong, W.C. (2022). "Economic and economic-statistical designs of variable sample size and sampling interval coefficient of variation chart", Communications in Statistics-Theory and Methods, Vol. 51 No. 6, pp.1811-1835. https://doi.org/10.1080/03610926.2020.1769670

Duncan, A.J. (1956). "The economic design of X charts used to maintain current control of a process", Journal of the American statistical association, Vol. 51 No. 274, pp.228-242. https://doi.org/10.1080/01621459.1956.10501322

Faraz, A. and Saniga, E. (2011). "Economic statistical design of a T2 control chart with double warning lines", Quality and Reliability Engineering International, Vol. 27 No. 2, pp.125-139. https://doi.org/10.1002/qre.1095

Ghanaatiyan, R., Amiri, A. and Sogandi, F. (2017). "Multi-objective economic-statistical design of VSSI-MEWMA-DWL control chart with multiple assignable causes", Journal of Industrial and Systems Engineering, Vol. 10, pp.34-58.

Huang, C.C. (2023). "Economic design of max charts using Taguchi's loss function", Communications in Statistics-Simulation and Computation, Vol. 52 No. 12, pp.6178-6192. https://doi.org/10.1080/03610918.2021.2009865

Jiao, J.R. and Helo, P.T. (2008). "Optimization design of a CUSUM control chart based on Taguchi's loss function", The international journal of advanced manufacturing technology, Vol. 35 No. 11, pp.1234-1243. https://doi.org/10.1007/s00170-006-0803-0

Katebi, M. and Khoo, M.B. (2021). "Optimal economic statistical design of combined double sampling and variable sampling interval multivariate T2 control charts", Journal of Statistical Computation and Simulation, Vol. 91 No. 10, pp.2094-2115. https://doi.org/10.1080/00949655.2021.1885669

Katebi, M., Seif, A. and Faraz, A. (2017). "Economic and economic-statistical designs of the T2 control charts with SVSSI sampling scheme", Communications in Statistics-Theory and Methods, Vol. 46 No. 20, pp.10149-10165. https://doi.org/10.1080/03610926.2016.1231823

Khaw, K.W., Khoo, M.B., Yeong, W.C. and Wu, Z. (2017). "Monitoring the coefficient of variation using a variable sample size and sampling interval control chart", Communications in Statistics-Simulation and Computation, Vol. 46 No. 7, pp.5772-5794. https://doi.org/10.1080/03610918.2016.1177074

Khoo, M.B., See, M.Y., Chong, N.L. and Teoh, W.L. (2019). "An improved variable sample size and sampling interval S control chart", Quality and reliability engineering international, Vol. 35 No. 1, pp.392-404. https://doi.org/10.1002/qre.2407

Lorenzen, T.J. and Vance, L.C. (1986). "The economic design of control charts: a unified approach", Technometrics, Vol. 28 No. 1, pp.3-10. https://doi.org/10.2307/1269598

Mirabi, M., Fatemi Ghomi, M.T. and Jolai, F. (2021). "Hybrid genetic algorithm for the economic-statistical design of variable sample size and sampling interval x-bar control chart", Journal of Industrial Engineering and Management Studies, Vol. 8 No. 2, pp.160-174. https://doi.org/10.22116/jiems.2022.138128

Niaki, S.T.A., Ershadi, M.J. and Malaki, M. (2010). "Economic and economic-statistical designs of MEWMA control charts—a hybrid Taguchi loss, Markov chain, and genetic algorithm approach", The International Journal of Advanced Manufacturing Technology, Vol 48, pp.283-296. https://doi.org/10.1007/s00170-009-2288-0

Pourtaheri, R. (2021). "Economic Statistical Design for Three-level Control Charts with Variable Sample Size", Sankhya B, pp.1-16. https://doi.org/10.1007/s13571-021-00249-y

Rafiei, N. and Asadzadeh, S. (2022). "Designing a risk-adjusted CUSUM control chart based on DEA and NSGA-II approaches A case study in healthcare: Cardiovascular patients", Scientia Iranica, Vol. 29 No. 5, pp.2696-2709. https://doi.org/10.24200/SCI.2020.54743.3895

Rafiei, N., Asadzadeh, S. and Niaki, S.T.A. (2023). "Multi-objective design of risk-adjusted control chart in healthcare systems with economic and statistical considerations", Communications in Statistics-Simulation and Computation, Vol. 52 No. 7, pp.2967-2984. https://doi.org/10.1080/03610918.2021.1923744

Reynolds, M.R., Amin, R.W., Arnold, J.C. and Nachlas, J.A. (1988). "$\bar{X}$ Charts with variable sampling intervals", Technometrics, Vol. 30 No. 2, pp.181-192. https://doi.org/10.2307/1270164

Safaei, A.S., Kazemzadeh, R.B. and Niaki, S.T.A. (2012). "Multi-objective economic statistical design of X-bar control chart considering Taguchi loss function", The International Journal of Advanced Manufacturing Technology, Vol. 59, pp.1091-1101. https://doi.org/10.1007/s00170-011-3550-9

Saghir, A., Hu, X., Tran, K.P. and Song, Z. (2023). "Optimal design and evaluation of adaptive EWMA monitoring schemes for inverse Maxwell distribution", Computers & Industrial Engineering, Vol. 181, p. 109290. https://doi.org/10.1016/j.cie.2023.109290

Saha, S., Khoo, M.B., Lee, M.H. and Haq, A. (2019). "A variable sample size and sampling interval control chart for monitoring the process mean using auxiliary information", Quality Technology & Quantitative Management, Vol 16 No. 4, pp.389-406. https://doi.org/10.1080/16843703.2018.1430523

Saniga, E.M. (1989). "Economic statistical control-chart designs with an application to and R charts", Technometrics, Vol. 31 No. 3, pp.313-320. https://doi.org/10.1080/00401706.1989.10488554

Tang, A., Sun, J., Hu, X. and Castagliola, P. (2019). "A new nonparametric adaptive EWMA control chart with exact run length properties", Computers & Industrial Engineering, Vol. 130 , pp.404-419. https://doi.org/10.1016/j.cie.2019.02.045

Xue, L., Wang, Q., Li, C. and An, L. (2025). "Economic design of residuals MEWMA control chart with variable sampling intervals and sample size", Communications in Statistics-Simulation and Computation, Vol 54 No. 2, pp.467-488. https://doi.org/10.1080/03610918.2023.2257008

Yeong, W.C., Tan, Y.Y., Lim, S.L., Khaw, K.W. and Khoo, M.B.C. (2024). "Variable sample size and sampling interval (VSSI) and variable parameters (VP) run sum charts for the coefficient of variation", Quality Technology & Quantitative Management, Vol. 21 No. 2, pp.177-199. https://doi.org/10.1080/16843703.2023.2177812

Yu, F.J. and Chen, H.K. (2009). "Economic-statistical design of X-bar control charts using Taguchi loss functions", IFAC Proceedings Volumes, Vol. 42 No. 4, pp.1719-1723. https://doi.org/10.3182/20090603-3-RU-2001.0098